PHYSICAL REVIEW B **68**, 054423 (2003)

Interconnected magnetoquantum de Haas–van Alphen oscillations in a two-dimensional metal: Wave form and Fourier harmonics

M. A. Itskovsky
Department of Chemistry, Technion–Israel Institute of Technology, Haifa, 32000, Israel

(Received 26 December 2002; revised manuscript received 31 March 2003; published 26 August 2003)

The theory of magnetoquantum oscillations in a two-dimensional (2D) metal with overlapping 2D and 1D energy bands, admitting multiple sets of closed and open orbits and a multisheet Fermi surface, is elaborated on. A system of coupled nonlinear equations for the chemical potential and magnetization oscillations is obtained in a level and harmonic representation. In the framework of a parametrical solution the resulting wave form of oscillation patterns, due to various fundamental frequencies interconnected through chemical potential oscillations, is calculated at any temperature and strength of reservoirs of magnetically unperturbed background states. Analytical expressions for renormalized Fourier harmonics of fundamental and combination frequencies (satellites of the higher frequency and its harmonics) are obtained dependent on the strength of the reservoir. The criterion of validity of these expressions as solutions of nonlinear equations is discussed. The symmetrization effect of the oscillation wave form is found in a multiband electron system without a reservoir of background states. It can be enhanced by the presence of a reservoir. The symmetrization effect is reflected via the nonstandard behavior of second harmonics: nonmonotonic temperature–magnetic-field dependence and disappearance at certain temperatures and magnetic fields (second harmonics zeros). Effects of this kind can also be revealed in heterostructures with external reservoirs of background states.

DOI: 10.1103/PhysRevB.68.054423 PACS number(s): 75.20.En, 75.30.Cr, 71.18.+y, 71.70.Di

I. INTRODUCTION

The phenomenon of magnetic quantum oscillations of magnetization and magnetoresistance [de Haas–van Alphen (dHvA)] and [Shubnikov–de Haas (SdH) effects] is widely utilized in establishing Fermi surfaces of metals.[1] The most important properties of metals, specific heat, electroconductivity, superconductivity, charge, spin density waves, etc., are determined by the details of their Fermi surface topology. Strongly anisotropic metals (such as recently synthesized organic conductors[2,3]) having relatively simple quasi-two-dimensional (2D) Fermi surfaces could be used as model crystals for checking various theoretical approaches describing magnetic quantum oscillations. In addition to the Fermi surface, the energy bands overlapping and the relative disposition of band edges also play an important role in influencing magnetic oscillation properties of metals. Generally, magnetic quantum oscillations in multiband 2D metals, admitting multiple fundamental frequencies, are strongly interconnected by the chemical potential oscillations. This results in the appearance of combination frequencies. A theoretical analysis of such magnetization oscillations in 2D metals with two energy bands, providing sets of closed orbits of electrons under high quantizing magnetic field, was undertaken by Alexandrov and Bratkovsky[4,5] and Nakano.[6] Their initial analysis was constrained by numerical calculations at zero temperature. Later the analytical expressions for Fourier harmonics of combination frequencies were obtained in an approximation of relatively high temperature[7] and for a model of two 2D bands with equal mass the theory has been extended to zero temperature.[8] Recently Kishigi and Hasegawa have numerically analyzed the expressions for dHvA oscillations in two 2D band electron systems applicable at any temperature.[9] The combination frequencies have been recently observed in uranium dipnictide $\mathrm{USb_2}$ (Ref. 10) and layered perovskite superconductor $\mathrm{Sr_2RuO_4}$,[11,12] both having cylindrical Fermi surfaces (similar to 2D metals). Combination frequencies have been also detected in multiband quantum-well heterostructure of InGaAs.[13]

In this work we will develop a theory of chemical potential and magnetization oscillations in multiband 2D metals having both closed and open Fermi surface sheets, the expressions obtained being applicable at arbitrary temperature. The presence of a reservoir of electrons situated on magnetically unperturbed background states [such as in open Fermi surface sheets and on impurity and defect levels (subbands)] will greatly influence the entire pattern of magnetic quantum oscillations. We will consider in detail an electron system consisting of two 2D bands and one 1D band which serves as a reservoir of background states. Under strong quantizing magnetic field the 2D bands provide closed electron orbits and 1D bands provide open ones (electronlike or holelike). It will be shown that due to the presence of reservoir states the effect of symmetrization of oscillations takes place: the wave form of oscillations will be symmetrized even at ultralow temperature as in one closed (2D) and one open (1D) band model considered in Ref. 14. The Fourier spectrum will be greatly influenced by the strength of the reservoir of background states. It will be characterized by the nonstandard nonmonotonic temperature dependence of second harmonics for electron systems with moderate reservoir strength. It will be shown that at certain temperature/magnetic field the second (even) harmonics may traverse the zero value (which is the manifestation of the symmetrization effect on magnetic quantum oscillations[15]). A stronger Fourier spectrum of combination frequencies is revealed at weaker strengths of the reservoir due to the stronger chemical potential oscillations. The symmetrization effect will also take place in a multiband electron system without reservoir. These effects under high quantizing magnetic fields will also take place in systems other than metal 2D electron systems, for example, in heterostructures with external reservoir of background states.

In Sec. II we will generalize the system of basic nonlinear equations for chemical potential and magnetization oscillations for multiband metals in the framework of level and harmonic approaches (developed in detail for one 2D band and one 1D band in Refs. 16 and 15). The model of multiband structure with two 2D bands and one 1D band will be elaborated and the strength of reservoir of background states presented by a transfer parameter calculated. In Sec. III A the wave form of interconnected oscillations will be calculated via the parametrical method[14] at various reservoir strengths. In Sec. III B the Fourier harmonics of fundamental and combination frequencies of magnetization oscillations in the presence of reservoir of background states will be derived and the validity of the obtained analytical expressions discussed. The effect of the symmetrization of oscillations wave form reflected by the temperature/magnetic field behavior of second harmonics of fundamental frequencies will be considered. In the Conclusion the comparison of theoretical results with available experimental Fourier spectrum in multiband electron systems is briefly discussed.

II. BASIC EQUATIONS FOR CHEMICAL POTENTIAL AND MAGNETIZATION OSCILLATIONS

A. Model

We consider here a model of a strongly anisotropic crystal (quasi-two-dimensional) having two two-dimensional (2D) energy bands overlapping with a 1D band (Fig. 1). There can be two situations: first, when one or two valence electrons on an unit cell fill the bottoms of the two 2D bands (forming electron pockets) and the bottom of the 1D band (electron pocket), and second, when two valence electrons on a unit cell fill the bottoms of the two 2D bands (electron pockets) and the 1D band, leaving a hole pocket near the ceiling of the 1D band. In the first model the whole number of electrons, conserved in the bottoms of the three upper bands, is fixed, in the second, the number of electrons in electron pockets of the two 2D bands is dependent on overlapping energy and may be arbitrary (as in compensated metal). The second model is reminiscent of the band structure of organic conductors[2] and will be considered here in detail. All results inhering to this model will also be valid for the first one, with the exception of the expression for the Fermi energy level (in the absence of magnetic field) and transfer parameter (describing the strength of reservoir). In both cases the Fermi surface consists of two closed and one open 2D sheets, corresponding to two Fermi surface cylinders (represented by two 2D bands) and a plain sheet (represented by the 1D band, will be called a sheet from here on).

Under high quantizing magnetic field electrons move along closed orbits, filling the corresponding quasiclassical energy levels [Landau levels (LL's)] in the 2D bands:

$$\varepsilon_{l_s}(B)=\hbar\omega_s(B)(l_s+1/2)+\Delta_s, \quad s=1,2 \tag{1}$$

(where $l_s=0,1,\ldots,$ designates quantized energy levels) and along open orbits (unperturbed by magnetic field where the spin splitting is neglected), filling the background reservoir states, which near the maximum (top) of the 1D band Δ could be represented as parabolic holelike ones (see Fig. 1)

$$\epsilon_{\mathbf{k}}=\Delta-\hbar^2(k_y-\pi/b^*)^2/2m_{sh}. \tag{2}$$

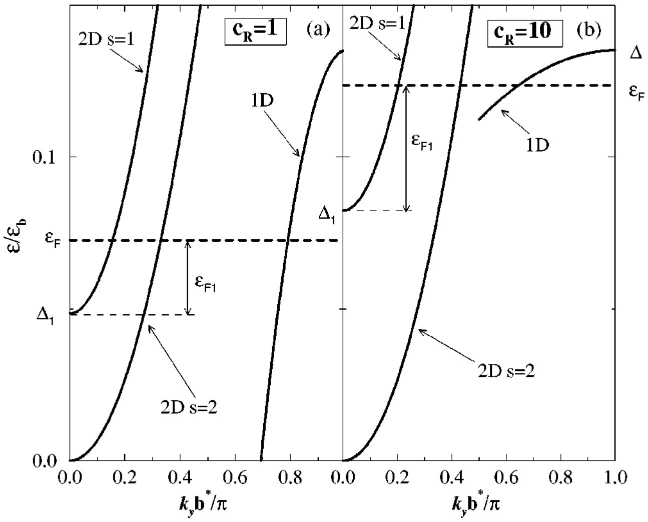

FIG. 1. Scheme of the dispersion in multiband energy structures consisting of two 2D bands overlapping with a 1D band. For simplicity, dispersion isotropic in the *xy* plain is shown for 2D bands. The top of the 1D band is situated at the $k_y=\pi/b^*$ Brillouin zone line. The Fermi surface consists of two cylinders and two plain sheets. Energies are counted off the bottom of the second $(s=2)$ 2D band, Δ_1 is the bottom of the first $(s=1)$ 2D band, Δ is the ceiling of the 1D band (overlapping energy), ε_F is the Fermi energy (or Fermi level, which is common to all bands), ε_{F1} is the Fermi energy of the first band, k_y is the wave vector component and b^* is the lattice constant in the y direction. The parameters used are as follows. The effective mass of the second band is $m_2/m_e=1.5$ (m_e is the electron mass), that of the first band is $m_1=m_2/1.5$. The Fermi energy ratio is $\varepsilon_{F1}/\varepsilon_F=1/3$ (which corresponds to the fundamental frequency ratio $F_2/F_1=4.5$), $\Delta/D_2=1/2$ $[D_2\equiv\hbar^2(2/b^*)^2/2m_2$ is the second band width in the k_y direction]. All energies are in ε_b units: $\varepsilon_b\equiv\hbar^2(\pi/b^*)^2/2m_e$ (at $b^*=10$ Å $\varepsilon_b\approx376$ meV). The band structure in (a) corresponds to the effective mass of the 1D band $m_{sh}=0.7m_e$ and transfer parameter $c_R\approx1$ (moderate strength 1D reservoir), in (b) $m_{sh}=11m_e$ and $c_R\approx10$ (strong 1D reservoir).

In Eq. (1) $\omega_s(B)=eB/m_sc$ is the cyclotron frequency corresponding to the cyclotron mass m_s of the s energy band (here $s=1,2$ with $s=1$ denoting the upper 2D band and $s=2$ that of the lower one, see Fig. 1) and Δ_s are the 2D bands bottom edges. All energies are counted from the bottom edge of the $s=2$ band $\Delta_2=0$. In this case the upper edge of the 1D band Δ stands for the overlapping energy. In the Eq. (2) k_y is the y component of the wave vector, b^* is the corresponding lattice constant [expression (1) includes anisotropy in the *xy* plain: $m_s=\sqrt{m_{sx}m_{sy}}$ (m_{sx}, m_{sy} are components of the effective mass tensor in the *xy* plain), certainly, the anisotropy in the z direction (anisotropic axis) is much stronger, leading to the 2D crystal]. m_{sh} is the absolute value of the hole mass tensor component in the k_y direction (which is for the holelike open plain sheet of the Fermi surface, arising from the 1D band, is negative). In considered case the number of electrons inside electron pockets is equal to the number of holes in a hole pocket of the hole sheet and is independent on magnetic field.

Thermodynamic potential for the considered model can be written as

$$\Omega(B,\zeta)=\Omega_{LL}(B,\zeta)+\Omega_R(\zeta), \tag{3}$$

$$\Omega_{LL}(B,\zeta)/AV = -k_BTB\sum_{s=1}^{2}\sum_{l_s=0}\ln(1+\exp\{[\zeta-\varepsilon_{l_s}(B)]/k_BT\}), \tag{4}$$

$$\Omega_R(\zeta)/V=-2k_BT\sum_{\mathbf{k}}\ln\{1+\exp[(\zeta-\varepsilon_{\mathbf{k}})/k_BT]\}, \tag{5}$$

where $\Omega_{LL}(B,\zeta)$ represents thermodynamic potential of electrons filling magnetically quantized states, Eq. (1).

$\Omega_R(\zeta)$ is the one due to electrons filling magnetically unperturbed states $\varepsilon_{\mathbf{k}}$ [near the ceiling of this 1D band being holelike, Eq. (2)], $A=2\cos\Theta/c^*\phi_0$ ($\phi_0=hc/e$ is the flux quantum, c^* is the lattice constant in the anisotropic direction of a 2D metal, and Θ is the tilt angle between anisotropic axis $\mathbf{c}^*$ and magnetic induction vector $\mathbf{B}$), ζ is the chemical potential generally dependent on magnetic field, and V is the crystal volume.

B. Nonlinear equation for chemical potential oscillations

First of all we obtain in the framework of considered model the equation for the chemical potential in the case of three overlapping bands (for one 2D and one 1D overlapping bands see Ref. 16):

$$n_{LL}(B,\zeta)=p_{sh}(\zeta), \tag{6}$$

where $n_{LL}(B,\zeta)=-\partial\Omega_{LL}(B,\zeta)/\partial\zeta$ is the concentration of electrons filling the two 2D bands electronlike pockets and

$$p_{sh}(\zeta)=\frac{1}{\upsilon\sqrt{\varepsilon_{sh}}}\int_0^\infty\{1+\exp[(\zeta-\Delta+\varepsilon)/k_BT]\}^{-1}\frac{d\varepsilon}{\sqrt{\varepsilon}}, \tag{7}$$

is the hole concentration in the 1D band holelike pocket [$\varepsilon_{sh}\equiv\hbar^2(\pi/b^*)^2/2m_{sh}$]. Equation (6) is obtained from expression for total concentration of electrons filling all three overlapping bands: $n_t=n_{LL}(B,\zeta)+n_{sh}(\zeta)$ [where $n_{sh}(\zeta)=-\partial\Omega_R(\zeta)/\partial\zeta$ is the electron concentration in the 1D band] by substitution: $n_t-n_{sh}(\zeta)=p_{sh}(\zeta)$. The total concentration of electrons filling the three overlapping bands $n_t=2/\upsilon$ (where ν is the unit cell volume) is obviously magnetic field independent.

Following the method derived in Refs. 14 and 16 [the level approach (LA)] from Eq. (6) we obtain an equation for chemical potential oscillations $\tilde{\zeta}(B,T)=\zeta(B,T)-\varepsilon_F$:

$$-\sum_{s=1}^{2}\frac{b_s}{2b_{n_s}}=\sum_{s=1}^{2}g(x_s,Q_s)+\frac{c_R}{\hbar\omega_1}\tilde{\zeta}, \tag{8}$$

where for $s=1,2$

$$-\frac{b_s}{2b_{n_s}}=\frac{F_s}{B}-\frac{F_s}{B_{n_s}},\quad b_s\equiv B-B_{n_s},\quad 2b_{n_s}=\frac{BB_{n_s}}{F_s}, \tag{9}$$

$$g(x_s,Q_s)=\frac{1}{1+\exp(x_s)}-\sum_{k=1}^{n_s}\frac{\sinh(x_s)}{\cosh(x_s)+\cosh(kQ_s)}, \tag{10}$$

$$Q_s(B,T)=\frac{\hbar\omega_s(B)}{k_BT},\quad F_s=\frac{\varepsilon_{Fs}}{\mu_s},\quad \mu_s\equiv\frac{e\hbar}{m_sc}, \tag{11}$$

where F_s are the fundamental frequencies of oscillations [F_1 is the low frequency characterizing the $s=1$ 2D band, F_2 is the high frequency characterizing the $s=2$ 2D band (both bands give closed 2D Fermi surface sheets constraining the electron pockets, see Fig. 1)], $2b_{n_s}$ are quasiperiods, corresponding to fundamental frequencies F_s, $Q_s(B,T)$ are the temperature smoothing parameters. The parametrical variables x_s are defined as

$$x_s(B,T)\equiv\varepsilon_{n_s}(B)-\zeta(B,T)/k_BT,\quad s=1,2,$$

and can be written via temperature smoothing parameters $Q_s(B,T)$ and chemical potential oscillations $\tilde{\zeta}(B,T)$ as

$$\frac{2x_s}{Q_s}=1+\frac{b_s}{b_{n_s}}-\frac{2}{\hbar\omega_s}\tilde{\zeta},\quad s=1,2. \tag{12}$$

Magnetic fields B_{n_s} are defined so that the corresponding quantized levels with quantum numbers n_s and n_s-1 are situated on equal distances from Fermi level, the magnetic fields B_{n_s} being in this case the points of symmetry for corresponding disposition of quantized levels: the filling of electrons on the upper level is equal to filling of holes on the underlying level on the same energetic distance from the Fermi level that the upper one. This symmetry provides the basis of level approach (LA) [level representation (LR) of $g(x_s,Q_s)$ function[14]].

The strength of reservoir of background states is determined by the transfer parameter c_R which in considered here case is defined relatively to the cyclotron mass of the first ($s=1$) 2D band:

$$c_R=\mu_1|\partial p_{sh}(\zeta)/\partial\zeta|_{\varepsilon_F}/A,\quad \mu_1=e\hbar/m_1c. \tag{13}$$

Substituting the relations b_s/b_{n_s} ($s=1,2$) from Eqs. (12) into Eq. (8) we obtain chemical potential oscillations via parametrical variables x_1 and x_2 in the level representation (LR) [$g(x_s,Q_s)$ function is the sum on pairs of quantized levels symmetrical relatively to the Fermi level in a separated large and small periods defined respectively by magnetic fields B_{n_1+1} and B_{n_1} and B_{n_2+1} and B_{n_2}]:

$$2\left(\sum_{s=1}^{2}\frac{1}{\hbar\omega_s}+\frac{c_R}{\hbar\omega_1}\right)\tilde{\zeta}(x_1,x_2)=\sum_{s=1}^{2}\left(1-2g(x_s,Q_s)-\frac{2x_s}{Q_s}\right). \tag{14}$$

Using the universal relation derived in Ref. 15

$$1-2g(x_s,Q_s)-\frac{2x_s}{Q_s}=\sum_{j_s=1}\tilde{m}_{j_s}(Q_s)\sin(2\pi j_s x_s/Q_s),$$

$$s=1,2, \tag{15}$$

$$\tilde{m}_{j_s}(Q_s)=\frac{4\pi}{Q_s\sinh(j_s 2\pi^2/Q_s)}, \tag{16}$$

we obtain the harmonic representation (HR) of chemical potential oscillations (the sum is now on Fourier harmonics)

$$2\left(\sum_{s=1}^{2}\frac{1}{\hbar\omega_s}+\frac{c_R}{\hbar\omega_1}\right)\tilde{\zeta}(x_1,x_2)$$

$$=\sum_{s=1}^{2}\sum_{j_s=1}\tilde{m}_{j_s}(Q_s)\sin(2\pi j_s x_s/Q_s). \tag{17}$$

Substituting x_s from Eqs. (12) into this equation we finally obtain the nonlinear equation for chemical potential oscillations in the harmonic representation

$$2\left(\sum_{s=1}^{2}\frac{1}{\hbar\omega_s}+\frac{c_R}{\hbar\omega_1}\right)\tilde{\zeta}(B,T)$$

$$=\sum_{s=1}^{2}\sum_{j_s=1}(-1)^{j_s+1}\tilde{m}_{j_s}(Q_s)$$

$$\times\sin\left\{j_s\left[2\pi\frac{F_s}{B}+\pi\frac{2\tilde{\zeta}(B,T)}{\hbar\omega_s}\right]\right\}$$

$$=\sum_{s=1}^{2}\sum_{j_s=1}(-1)^{j_s}\tilde{m}_{j_s}(Q_s)\sin\left\{j_s\left[k_s b_s-\pi\frac{2\tilde{\zeta}(B,T)}{\hbar\omega_s}\right]\right\}. \tag{18}$$

To obtain the second line of Eq. (18) we used the definition of magnetic fields B_{n_s} at which the mean line between Landau levels with quantum numbers n_s and n_s-1 is crossing the Fermi level ε_F:

$$F_s=n_s B_{n_s}, \quad s=1,2. \tag{19}$$

In the third line of Eq. (18) $k_s=2\pi/2b_{n_s}$ is the cyclic frequency with respect to the variable $b_s=B-B_{n_s}$. The "Fermi energy" of the corresponding energy band is defined as $\varepsilon_{Fs}=\varepsilon_F-\Delta_s$ [see Fig. 1, where the bottom edge of the second 2D band ($s=2$) is taken as zero energy level $\Delta_2=0$ and therefore $\varepsilon_{F2}\equiv\varepsilon_F$]. "Fermi energies" can also be expressed as $\varepsilon_{Fs}=\mu_s F_s=\mu_s n_s B_{n_s}=\hbar\omega_s(B_{n_s})n_s$. This being taken into account, in the used throughout this paper approximation for appropriate magnetic fields $B/F_s\cong B_{n_s}/F_s=\hbar\omega_s/\varepsilon_{Fs}\ll 1$, the large (for 2D band $s=1$) and small (for 2D band $s=2$) period of oscillations can be represented as $2b_{n_s}=BB_{n_s}/F_s\cong B_{n_s+1}B_{n_s}/F_s\cong B^2_{n_s}/F_s$ and, hence, the cyclic frequencies corresponding to these periods are $k_s\cong 2\pi F_s/B^2_{n_s}$.

C. Magnetization oscillations

Acting in the framework of the level approach (LA) elaborated in detail in Refs. 14 and 16 we obtain expression for magnetization oscillations for our model as a function of parametrical variables x_s

$$\frac{M(x_1,x_2)}{M_0}=\sum_{s=1}^{2}\frac{\varepsilon_{Fs}}{\varepsilon_F}\left[1-2g(x_s,Q_s)-\frac{2x_s}{Q_s}\right], \tag{20}$$

where $M_0=A\varepsilon_F/2$ is the saturation magnetization of the deepest quantized band (the second 2D band is $s=2$, in our case we have designated $\varepsilon_F\equiv\varepsilon_{F2}\geqslant\varepsilon_{F1}$, see Fig. 1).

This is the level representation (LR) of magnetization oscillations via parametrical variables x_s. The deposition of each quantized band into the total magnetization is determined by the corresponding "weight" factor, the Fermi energy ε_{Fs}. Comparing this expression with that of the chemical potential oscillations (14), we now see that magnetization oscillations are nonproportional to the chemical potential oscillations [as was the case in the presence of a single quantized band (see the Refs. 14 and 16)]. Only in a special case when the bottoms of quantized 2D bands coincide (degenerate) ($\Delta_1=\Delta_2$, that is, $\varepsilon_{F1}=\varepsilon_{F2}\equiv\varepsilon_F$, see Fig. 1) the proportionality relation preserves.

Using the identity (15), (16), we obtain magnetization oscillations in the harmonic representation (HR) via parametrical variables x_s:

$$\frac{M(x_1,x_2)}{M_0}=\sum_{s=1}^{2}\frac{\varepsilon_{Fs}}{\varepsilon_F}\sum_{j_s=1}\tilde{m}_{j_s}(Q_s)\sin(2\pi j_s x_s/Q_s). \tag{21}$$

As in a case with chemical potential oscillations the magnetization oscillations can be represented as functions both of inverse magnetic field ($1/B$) and magnetic field ($b_s=B-B_{n_s}$) by substituting the parametrical variables x_s via Eqs. (12):

$$\frac{M(B,T)}{M_0}=\sum_{s=1}^{2}\frac{\varepsilon_{Fs}}{\varepsilon_F}\sum_{j_s=1}(-1)^{j_s+1}\tilde{m}_{j_s}(Q_s)$$

$$\times\sin\left\{j_s\left[2\pi\frac{F_s}{B}+\pi\frac{2\tilde{\zeta}(B,T)}{\hbar\omega_s}\right]\right\}$$

$$=\sum_{s=1}^{2}\frac{\varepsilon_{Fs}}{\varepsilon_F}\sum_{j_s=1}(-1)^{j_s}\tilde{m}_{j_s}(Q_s)$$

$$\times\sin\left\{j_s\left[k_s b_s-\pi\frac{2\tilde{\zeta}(B,T)}{\hbar\omega_s}\right]\right\}. \tag{22}$$

Now we see that magnetization oscillations can be obtained by solving firstly the nonlinear equation for the chemical potential oscillations: Eq. (14) with Eq. (12) in level representation (LR) or Eq. (18) in harmonic representation (HR) that will be done in the next section. If we completely neglect chemical potential oscillations $\tilde{\zeta}(B,T)\equiv 0$, the expression in Eq. (22) reduces to Lifshitz-Kosevich formula[17] for two quantized independent 2D bands (for single 2D band this formula was obtained by Shoenberg[18]).

D. Transfer parameter for overlapping bands

The electrons filling magnetically unperturbed states in nonquantized 1D band implicitly influence magnetization oscillations via participation in the chemical potential oscillations which are depending explicitly on the transfer parameter c_R [see nonlinear equation for the chemical potential oscillations, Eq. (14) in level representation or Eqs. (17), (18) in harmonic representation]. This parameter as defined by Eq. (13) is determined by the $B=0$ band structure. The Fermi level can be found from Eq. (6) at $B=0$:

$$\frac{\varepsilon_F}{\mu_2}+\frac{\varepsilon_F-\Delta_1}{\mu_1}=\frac{p_{sh}(\varepsilon_F)}{A}, \tag{23}$$

with μ_s $(s=1,2)$ from Eq. (11).

The degenerate hole concentration inside the hole pocket of the 1D band is obtained from Eq. (7):

$$p_{sh}(\zeta)\cong\frac{1}{v\sqrt{\varepsilon_{sh}}}(\Delta-\zeta)^{1/2}. \tag{24}$$

Solving Eq. (23) we obtain Fermi energy in our model:

$$\frac{\varepsilon_F}{\varepsilon_b}=\frac{4}{\pi^2}\frac{m_{sh}}{m_2}\frac{1}{m_2/m_e}\times\left[\frac{\sqrt{1+4(1+F_1/F_2)^2\Delta/\varepsilon_{ef}}-1}{2(1+F_1/F_2)^2}\right], \tag{25}$$

where

$$\Delta/\varepsilon_{ef}\equiv(\Delta/D_2)(m_2/m_{sh}),\quad \frac{F_1}{F_2}=\frac{m_1\varepsilon_{F1}}{m_2\varepsilon_F}, \tag{26}$$

$$\varepsilon_b=\frac{\hbar^2(\pi/b^*)^2}{2m_e},\quad D_2=\frac{2\hbar^2(b^*)^{-2}}{m_2}=\frac{(4/\pi^2)\varepsilon_b}{m_2/m_e},$$

D_2 is the width of the second 2D band $(s=2)$ in the k_y direction. For parabolic band approximation being true, obviously, the overlapping should be $\Delta/D_2\lesssim 1/2$ (see Fig. 1).

Now the transfer parameter calculated in the considered model is

$$c_R=\frac{(m_2/m_1)(1+F_1/F_2)}{\sqrt{1+4(1+F_1/F_2)^2\Delta/\varepsilon_{ef}}-1}. \tag{27}$$

Hence, the transfer parameter is determined by the four parameters m_2/m_1, m_2/m_{sh}, $\varepsilon_F/\varepsilon_{F1}$ (or F_1/F_2 as $F_1/F_2=m_1\varepsilon_{F1}/m_2\varepsilon_F$), and Δ/D_2.

The transfer parameter for a model consisting of two bands, one 2D band with an electron pocket and one 1D band also with an electron pocket, was calculated in Ref. 14. c_R can be calculated in a way similar to two 2D bands and 1D band, all with electron pockets. The limit for $c_R\rightarrow 0$ in models with two 2D bands plus one 1D band depends on whether the 1D pocket is electronlike or holelike: in the first case the weak electronlike reservoir (containing a small number of carriers, for example, because of a small effective mass) means strong magnetization oscillations [with large amplitude M_0 because of large Fermi energies ε_{F1} and ε_F (corresponding to large numbers of electrons conserved in two 2D bands)]. In the second case (considered here) the weak holelike reservoir means extremely small magnetic oscillations due to the small number of carriers filling the 2D bands. Consequently, the holelike reservoir influences the magnetic oscillations more strongly than the electronlike one. But qualitatively the influence of the reservoir on magnetic quantum oscillations in both cases for the same value of $c_R\neq 0$ is the same.

It should be noted that the expressions for magnetization [Eqs. (20)–(22)] do not contain the transfer parameter c_R explicitly. Reservoir of background states influences the magnetization implicitly through chemical potential oscillations, (14), (17), (18). All expressions for magnetization and chemical potential oscillations, obtained here, are applicable independently of the concrete nature of the background state reservoir.

III. WAVE FORM AND FOURIER SPECTRUM IN THE PRESENCE OF RESERVOIR OF BACKGROUND STATES

A. Wave forms observed in oscillation pattern

The wave form of magnetization oscillations can be calculated at arbitrary temperature and any reservoir strength by application of expressions of the level representation [Eq. (20)] and harmonic representation [Eq. (21)], both dependent on parametrical variables x_s, without the necessity of solving the nonlinear equation for chemical potential oscillations (as these equations do not contain chemical potential oscillations explicitly). For a 2D crystal containing a single energy band and a reservoir of background states this procedure was described in Refs. 14,16. The parametrical variables should be given in certain limits of temperature smoothing parameters Q_s. For obtaining the wave form in a single large period corresponding to the low fundamental frequency F_1 (with variable x_1 ranging in the limits $-Q_1/2<x_1<Q_1/2$) the variable x_2 should be taken in the region $-(F_2/F_1)Q_2<x_2<(F_2/F_1)Q_2$ so as to cover several small periods corresponding to high fundamental frequency F_2. To show two large periods the regions of x_s should be doubled and so on. This parametrical method proved successful especially at ultralow temperature (large Q_s) when only a few levels in the g functions play the decisive role. The parametrical method provides the possibility of elucidating the role of the reservoir of the background nonquantized in magnetic field states. These results are shown in Fig. 2, where the presence of weak $(c_R\ll 1)$, intermediate $(c_R\sim 1-2)$, and strong $(c_R\gg 1)$ reservoirs of background states greatly influences the wave form of oscillations.

It is seen that the shape of high frequency oscillations (corresponding to fundamental frequency F_2) alters from

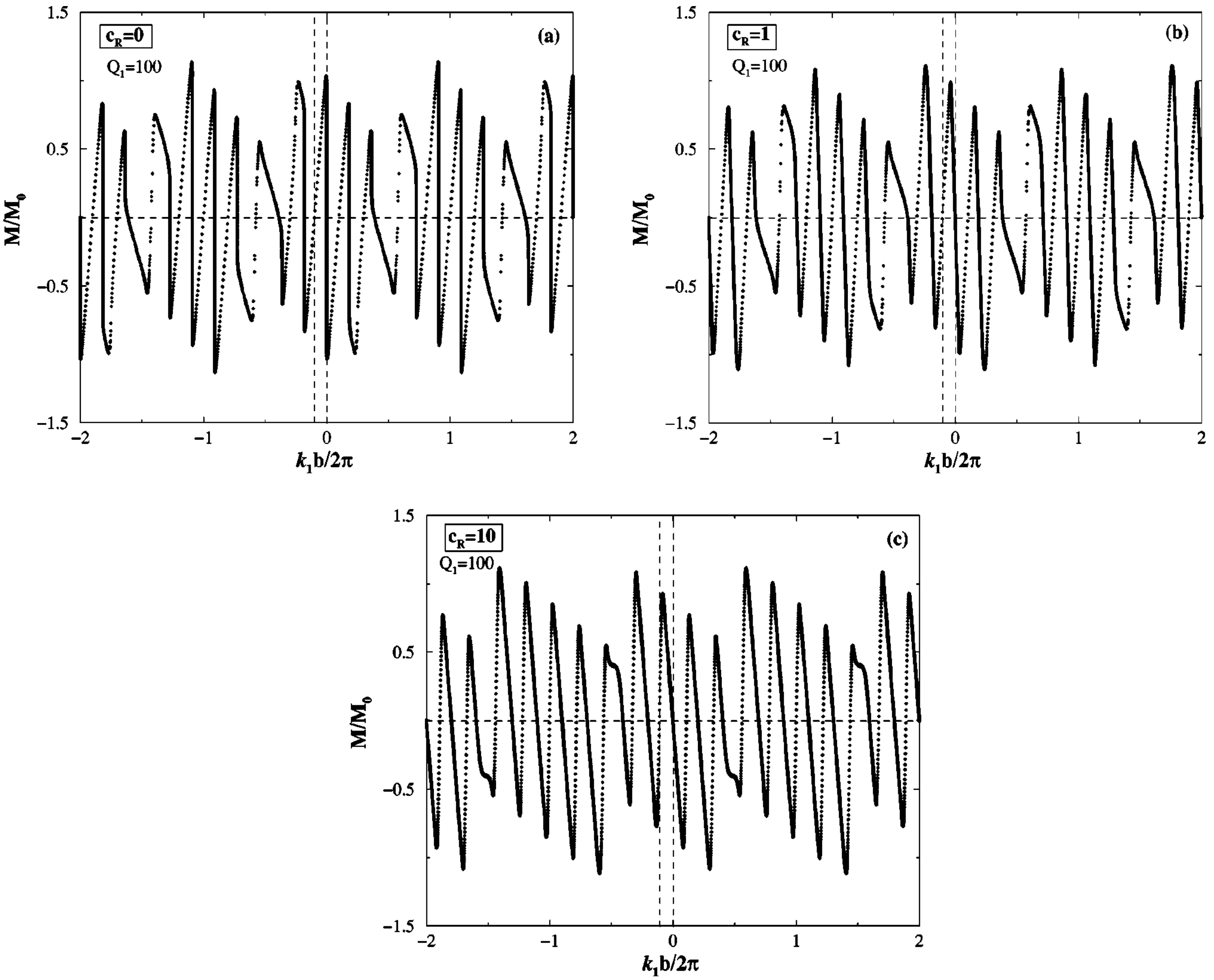

FIG. 2. Magnetization oscillations patterns in two 2D band electron systems at various strengths of 1D reservoirs of background states at ultralow temperature ($Q_1=100$): (a) transfer parameter $c_R=0$ (absence of reservoir), (b) $c_R=1$ (moderate strength reservoir), (c) $c_R=10$ (strong reservoir). The fundamental frequency ratio is $F_2/F_1=4.5$, the effective mass ratio is $m_2/m_1=1.5$ (these data correspond to a Fermi energy ratio $\varepsilon_{F1}/\varepsilon_F=1/3$). Four periods corresponding to low fundamental frequency F_1 are shown, corresponding to two large periods (with frequency $F_1/2$, see text). The half period corresponding to high fundamental frequency F_2 is separated by dashed lines. Inside it the change of the wave form of oscillations due to background states reservoir is manifested: from sawtooth [in (a) at $c_R=0$] through more symmetric [in (b) at $c_R=1$] to inverse sawtooth [in (c) at $c_R=10$].

sawtooth ($c_R \ll 1$) to inverse sawtooth ($c_R \gg 1$) in a symmetric pattern ($c_R \sim 1-2$). As in the case with a single quantized band background the states do not change the amplitudes of the oscillations. It is also seen from the wave form of the oscillations pattern that a new feature of the two 2D band system arises: the largest visible period of oscillations in the case of the fundamental frequency ratio given by the half-integer numbers $F_2/F_1=N/2$ ($N=3,5,\ldots$) is twice of the low frequency period and corresponds to the $F_1/2$ fundamental frequency. This case is provided in Fig. 2 for the ratio $F_2/F_1=4.5=9/2$. In the case of integer ratio $F_2/F_1=N(N=2,3,\ldots)$ the largest visible period is that of the low frequency F_1. This is illustrated in Fig. 3 for fundamental frequencies ratio $F_2/F_1=4$.

Generally, these properties follow from the expression for the fundamental frequencies ratio $F_2/F_1=B_{n_2}n_2/B_{n1}n_1$ [see the definition of magnetic fields B_{n_s}, Eqs. (19)] at the condition that magnetic fields where mean lines between levels with quantum numbers n_s and n_s-1 belonging to different bands ($s=1,2$) cross the Fermi level at one point: $B_{n_2}=B_{n_1}$, $F_2/F_1=n_2/n_1$. If the ratio $F_2/F_1=N/4$ ($N=5,7,\ldots$) the visible period of oscillations pattern will be four times of the low frequency period and correspond to fundamental frequency $F_1/4$. If $F_2/F_1=N/5$ and $F_2/F_1=N/10$ (where $N/5$ and $N/10$ are irreducible improper fractions) the corresponding visible period of the oscillation pattern will be 5 and 10 times of the low frequency period with fundamental frequencies $F_1/5$ and $F_1/10$. This exhausts the cases when the ratio F_2/F_1 is given with precision to tenths: $F_2/F_1=NL$ (N,L are integer numbers). For a ratio with more precision the greater visible periods can be constructed

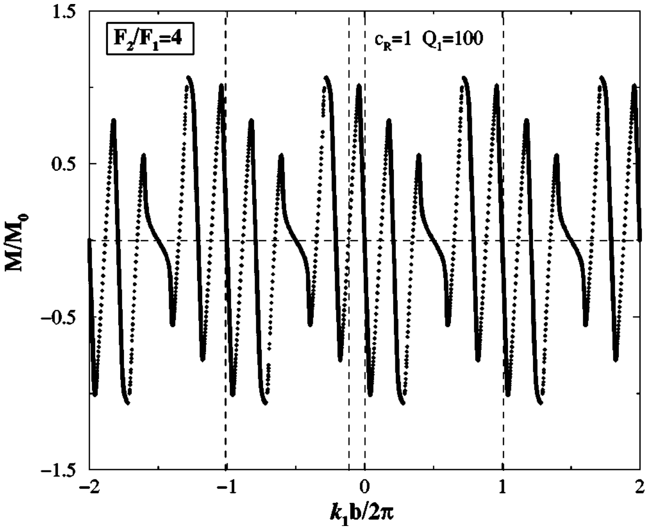

FIG. 3. The magnetization oscillation pattern in two 2D bands electron systems at an integer fundamental frequency ratio. Parameters used: fundamental frequencies ratio $F_2/F_1=4$, cyclotron mass ratio $m_2/m_1=1.5$, temperature smoothing parameter $Q_1=100$, transfer parameter $c_R=1$. Note that the visible period of the oscillation pattern completely coincides with that of the low fundamental frequency F_1. Four such periods are shown. A half period due to the high fundamental frequency F_2 is separated by dashed lines demonstrating the nearly symmetric wave form of oscillations due to the moderate strength $(c_R=1)$ 1D reservoir.

accordingly. While features influenced by background states are difficult to observe from the oscillation pattern itself the Fourier spectrum will be a much more powerful tool.

B. Fourier spectrum

For analytically obtaining the Fourier spectrum of magnetization in two quantized bands and a reservoir of background states model the nonlinear equation for chemical potential oscillations should be solved first and then this solution should be substituted into the expression for magnetization. Such a problem is very difficult to perform. For a simple model of a single quantized band in the presence of a reservoir of background states this problem was solved in Ref. 15 taking into account the spin splitting at $T=0$ in Ref. 19. Here for obtaining the Fourier spectrum at arbitrary temperature (including ultralow temperatures corresponding to large $Q_s \gg 10$) we solve the nonlinear equation for chemical potential oscillations numerically.

At high temperature $(Q_s \lesssim 10)$ we solve the problem analytically obtaining explicit expressions for Fourier harmonics. A similar solution in the multiband system without reservoir states was presented in Ref. 7. Further discuss the conditions for such a solution which appeared to be better applicable in the high-temperature–low-magnetic field region and for electron systems with stronger reservoirs.

The Fourier spectrum of magnetization oscillations in a two 2D band system without $(c_R=0)$ and with moderate $(c_R \sim 1)$ and strong $(c_R \gtrsim 10)$ reservoirs of background states is presented in Fig. 4. In the absence of a reservoir and with moderate reservoirs [see Figs. 4(a), 4(b)] the higher harmonics of both low F_1 and high F_2 fundamental frequencies $(j_s=2,3,\dots)$ are suppressed (see second harmonics $2F_1$ and $2F_2$), but combination frequencies $(F_2 \pm F_1,\ 2F_2+F_1,\ 2F_2+2F_1)$ are much stronger due to the substantial chemical potential oscillations present. In a system with a strong reservoir [see Fig. 4(c)] the second harmonics $2F_1$ and $2F_2$ are of the same order as the combination frequencies which are diminished in this case of suppressed chemical potential oscillations. Obviously, all these differences in the Fourier spectrum are mirrowing the changes in the symmetry of the wave form of the oscillation pattern (shown in Figs. 2, 3) reflecting in turn the influence of background reservoir states. Note that the suppression of second harmonics of fundamental frequencies is utmost in multiband systems without a reservoir reflecting the interference of 2D bands due to chemical potential oscillations which are strongest in this case. This effect of the second (even) harmonics suppression in multiband systems without a reservoir [see Fig. 4(a)] is of the same nature as revealed in electron systems consisting of a single band and reservoir (see Ref. 15): the symmetrization of the wave form of oscillations is due to chemical potential oscillations leading to the redistribution of electrons between bands (for the symmetrization effect in multiband systems see Figs. 6, 7 and the corresponding discussion).

Later we will solve the system of equations (18) (chemical potential oscillations) and (22) (magnetization oscillations) with conditions of relatively small amplitudes of chemical potential oscillations:

$$j_s\pi\frac{2\tilde{\zeta}(B,T)}{\hbar\omega_s}\lesssim 0.5,\quad s=1,2,\quad j_s=1,2,\dots \tag{28}$$

(when trigonometric functions entering into these equations can be substituted as $\cos x \cong 1$ and $\sin x \cong x$) obtaining the Fourier harmonics of fundamental and combination frequencies. Obviously, these conditions are better satisfied in systems with a larger ratio of quantized band mass m_2/m_1, stronger reservoir (larger transfer parameter c_R), and mainly at relatively small standard Lifshitz-Kosevich (LK) harmonics $\tilde{m}_{j_s}(Q_s)=(4\pi/Q_s)\sinh(j_s 2\pi^2/Q_s)$ which takes place at relatively high temperature $(Q_s \lesssim 10)$. It is obvious that restrictions from high frequency oscillations (representing the $s=2$ band) are tougher because of greater mass (and consequently, the lesser separation between levels $\hbar\omega_2 < \hbar\omega_1$).

In the linear on chemical potential oscillations approximation we obtain for magnetization

$$\frac{M(B,T)}{M_0}\cong\sum_{s=1}^{2}\frac{\varepsilon_{Fs}}{\varepsilon_F}\sum_{j_s=1}(-1)^{j_s}\tilde{m}_{j_s}(Q_s)\left\{\sin(j_s k_s b_s)-j_s\pi\frac{2\tilde{\zeta}(B,T)}{\hbar\omega_s}\cos(j_s k_s b_s)\right\}. \tag{29}$$

Substituting the expression for chemical potential oscillations (18), in which we neglect by chemical potential oscillations terms in the right-hand-side of Eq. (18) (in the arguments of trigonometric functions), into Eq. (29) and using the trigonometric relation $\sin(x)\cos(y)=(1/2)[\sin(x+y)+\sin(x-y)]$ we obtain a Fourier series for magnetization. In

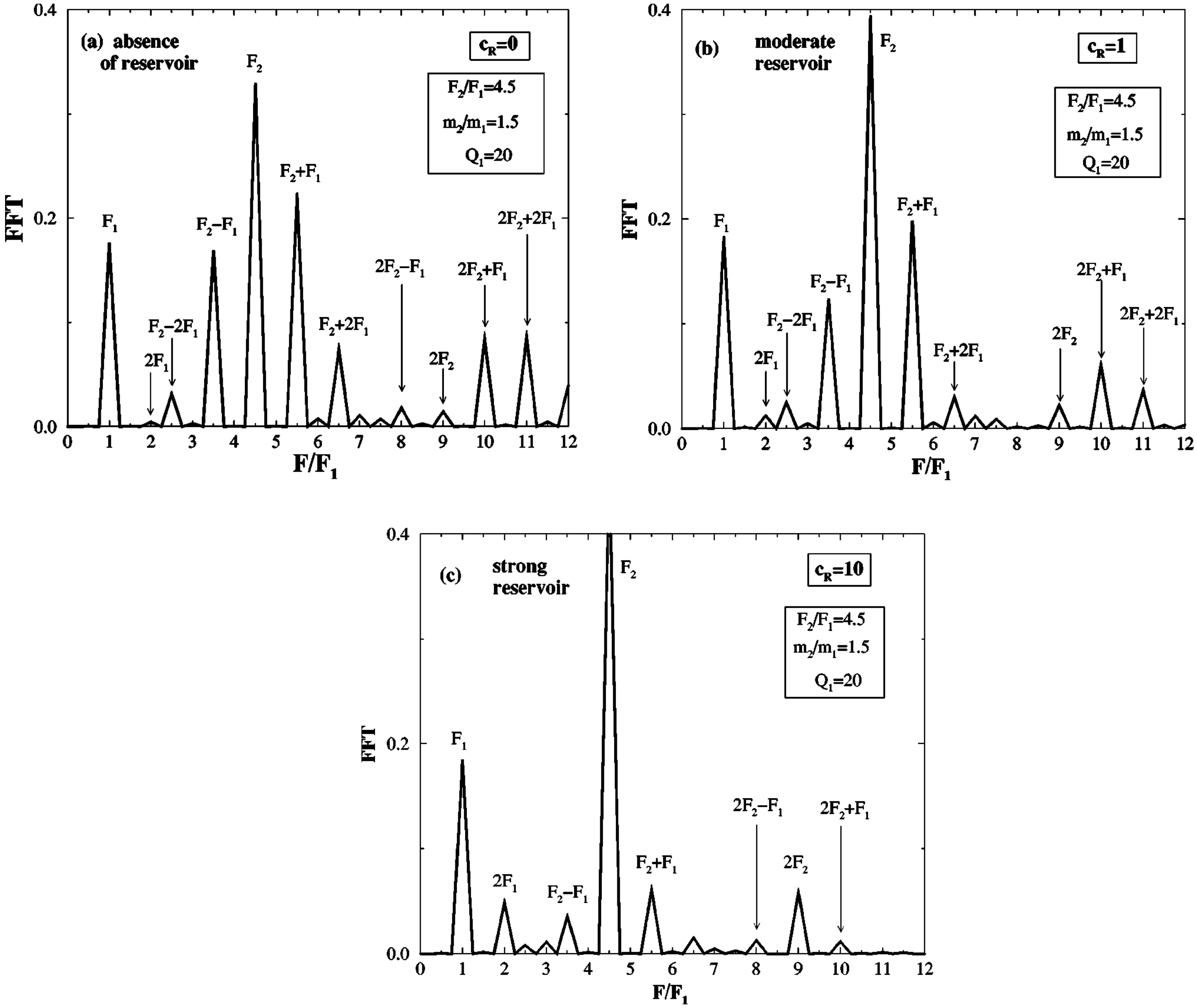

FIG. 4. Fourier transform of magnetization oscillations in two 2D bands electron systems: (a) in the absence of reservoir, (b) with moderate ($c_R=1$), and (c) strong ($c_R=10$) reservoir of background states. The fundamental frequency ratio $F_2/F_1=4.5$, cyclotron mass ratio $m_2/m_1=1.5$, temperature smoothing parameter $Q_1=20$. Note in (a) and (b) the strong harmonics of combination frequencies (first satellites F_2-F_1, F_2+F_1 and second satellites F_2-2F_1, F_2+2F_1 of the first harmonic of fundamental frequency F_2 and first $2F_2+F_1$ and second $2F_2+2F_1$ right satellites of the second harmonic $2F_2$ [in (a) also the first left satellite $2F_2-F_1$] and weak second harmonics of fundamental frequencies ($2F_1$ and $2F_2$). (c) The inverse situation with weak harmonics of combination frequencies and relatively strong second harmonics of fundamentals. Note the substantial suppression of second harmonics in (a) and (b) in comparison with those in (c).

this series will be represented together with renormalized harmonics of fundamental frequencies (meaning the standard LK harmonics $\tilde{m}_{j_s}(Q_s)$ [see Eq. (16)] plus additions due to chemical potential oscillations, expressed as powers on standard LK harmonics) also the harmonics of combination frequencies $j_{s'}k_{s'} \pm j_s k_s$ $(s' \neq s)$ (we remind the reader that $k_s \propto F_s$). Similarly, the higher chemical potential oscillation terms can be calculated providing the third and higher order terms on standard LK harmonics in the Fourier series.

We will not present simple but cumbersome general expressions for Fourier series on fundamental and combination frequencies [general solution of Eqs. (18), (22) in linear and a higher approximation on chemical potential oscillations $\tilde{\zeta}$]. Instead, we will provide expressions for the first and second renormalized harmonics of fundamental frequencies F_1 and F_2 and the harmonics of combination frequencies $j_2F_2 \pm j_1F_1$ ($j_1, j_2 = 1,2,\dots$) later.

1. First harmonics

The renormalized amplitude of the first harmonic of the low fundamental frequency F_1 ($j_1=1, s=1$)$M_1^{(F_1)}(Q_1)/M_0 = h_1^{(F_1)}(Q_1)\sin(k_1 b_1)$ is

$$h_1^{(F_1)}(Q_1) = -\frac{\varepsilon_{F1}}{\varepsilon_F}\left\{\tilde{m}_1(Q_1) + \frac{\pi \tilde{m}_1(Q_1)\tilde{m}_2(Q_1)}{2(1+m_2/m_1+c_R)} - \frac{\pi^2[\tilde{m}_1(Q_1)]^3}{4(1+m_2/m_1+c_R)^2}\right\}, \tag{30}$$

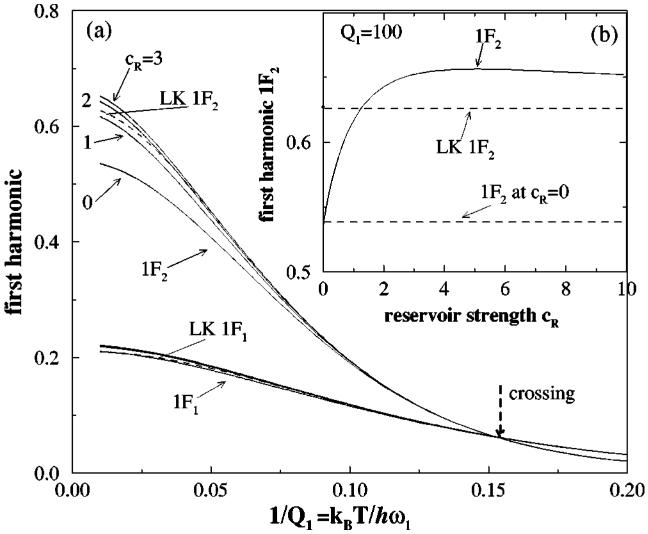

FIG. 5. (a) First harmonic amplitudes $[h_1^{(F_1)}(Q_1)\rightarrow 1F_1$ and $h_1^{(F_2)}(Q_2)\rightarrow 1F_2]$ of the low (F_1) and high (F_2) fundamental frequencies in electron system consisting of two 2D bands + a 1D reservoir of background states. For each fundamental frequency the curves from above correspond to transfer parameter $c_R=3,2,1,0$, LK harmonics $(\varepsilon_{F1}/\varepsilon_F)\tilde{m}_1(Q_1)\rightarrow \mathrm{LK}1F_1$ and $\tilde{m}_1(Q_2)\rightarrow \mathrm{LK}1F_2$ are shown by dashed lines. Note that curve $1F_2$, corresponding to $c_R=0$ at ultralow temperatures, is rather approximate [see criterion (28)]. The fundamental frequency ratio is $F_2/F_1=4.5$, the effective mass ratio is $m_2/m_1=1.5$, the Fermi energy ratio is $\varepsilon_{F1}/\varepsilon_F=1/3$. (b) First harmonic $1F_2$ of the high fundamental frequency F_2 versus strength of background states, represented by transfer parameter c_R, at temperature smoothing parameter $Q_1=100$. LK $1F_2$ (corresponding to $c_R\rightarrow\infty$) and $1F_2$ at $c_R=0$ are shown by dashed lines.

where the subscripts of $M_1^{(F_1)}, h_1^{(F_1)}$, and $\tilde{m}_1$ designate the number of harmonics ($j_1=1$), the subscripts of Q_1, F_1, m_1, j_1, and k_1 stand for the number of the first (low) fundamental frequency F_1 (band $s=1$), and the subscript for m_2, for the second band ($s=2$). It should be noted that the last term in braces was obtained when the terms proportional to $(\tilde{\zeta})^2$ were taken into account while solving the nonlinear equations.

The renormalized amplitude of the first harmonic of the high fundamental frequency F_2 ($j_2=1, s=2$) $M_1^{(F_2)}(Q_2)/M_0=h_1^{(F_2)}(Q_2)\sin(k_2b_2)$ is

$$h_1^{(F_2)}(Q_2)=-\left\{\tilde{m}_1(Q_2)+\frac{\pi(m_2/m_1)\tilde{m}_1(Q_2)\tilde{m}_2(Q_2)}{2(1+m_2/m_1+c_R)}\right.$$
$$\left.-\frac{\pi^2(m_2/m_1)^2[\tilde{m}_1(Q_2)]^3}{4(1+m_2/m_1+c_R)^2}\right\}. \tag{31}$$

The renormalized first harmonic amplitudes (30), (31) are shown in Fig. 5. Designations $h_1^{(F_1)}(Q_1)\rightarrow 1F_1$ and $h_1^{(F_2)}(Q_2)\rightarrow 1F_2$, $(\varepsilon_{F1}/\varepsilon_F)\tilde{m}_1(Q_1)\rightarrow LK1F_1$, and $\tilde{m}_1(Q_2)\rightarrow LK1F_2$ (for Lifshitz-Kosevich (LK) harmonics) are used and here and later the sign “→” stands for “designated as.”

It is seen [see Fig. 5(b)] that at low temperatures (large temperature smoothing parameter $Q_1=100$) the first harmonics nonmonotonically depend on the strength of background reservoir states: at a given temperature (or Q_1) with increasing reservoir strength c_R they first increase, then decrease reaching the limiting value of the LK ones [LK first harmonics $\tilde{m}_1(Q_1)$ and $\tilde{m}_1(Q_2)$ characterize the considered system with completely neglected chemical potential oscillations $\tilde{\zeta}(B,T)\equiv 0$, that can be asymptotically achieved in ultrastrong reservoirs of background states $c_R\rightarrow\infty$)]. This behavior reflects the symmetry of oscillation wave forms due to the various reservoir strengths.[14,15] At high temperatures the $1F_1$ becomes greater than $1F_2$ [see crossing in Fig. 5(a)] notwithstanding that it is presented with a smaller weight (smaller Fermi energy $\varepsilon_{F1}/\varepsilon_F=1/3$).

In pure two 2D band systems (i.e., without a reservoir) the first harmonics can be essentially suppressed only at low temperature [see the curve LK $1F_2$ at $c_R=0$ in Fig. 5(a)] reflecting the minimal symmetry of oscillations wave form in this case [sawtooth, see Fig. 2(a)].

In general, the first harmonics at moderate and high temperatures ($Q_1\lesssim 20$) are slightly affected by the interference of 2D bands and by the reservoir of background states. Therefore, the cyclotron masses obtained from LK first harmonics in this temperature range are reasonable (excluding the special case of two 2D bands without reservoir [see the first harmonic $1F_2$ for $c_R=0$ at low temperatures ($Q_1 \gtrsim 20$) in Fig. 5(a)].

2. Nonstandard temperature/magnetic field dependence of second harmonics

Renormalized amplitude of the second harmonic of the low fundamental frequency F_1 ($j_1=2, s=1$) $M_2^{(F_1)}(Q_1)/M_0 = h_2^{(F_1)}(Q_1)\sin(2k_1b_1)$ is

$$h_2^{(F_1)}(Q_1)=\frac{\varepsilon_{F1}}{\varepsilon_F}\left\{\tilde{m}_2(Q_1)-\frac{\pi[\tilde{m}_1(Q_1)]^2}{2(1+m_2/m_1+c_R)}\right\}. \tag{32}$$

The renormalized amplitude of the second harmonic of the high fundamental frequency F_2 ($j_2=2, s=2$) $M_2^{(F_2)}(Q_2)/M_0=h_2^{(F_2)}(Q_2)\sin(2k_2b_2)$ is

$$h_2^{(F_2)}(Q_2)=\tilde{m}_2(Q_2)-\frac{\pi(m_2/m_1)[\tilde{m}_1(Q_2)]^2}{2(1+m_2/m_1+c_R)}. \tag{33}$$

The second harmonic amplitudes $h_2^{(F_1)}(Q_1)\rightarrow 2F_1$ and $h_2^{(F_2)}(Q_2)\rightarrow 2F_2$, Eqs. (32), (33), can be decreased substantially, compared with LK second harmonics $(\varepsilon_{F1}/\varepsilon_F)\tilde{m}_2(Q_1)\rightarrow \mathrm{LK}2F_1$ and $\tilde{m}_2(Q_2)\rightarrow \mathrm{LK}2F_2$, in a certain interval of temperatures because they contain the square of the unrenormalized (LK) first harmonic amplitudes in their negative term. This effect of diminishing of the absolute value of the second harmonic and even becoming zero at certain temperature/magnetic fields was first predicted to oc-

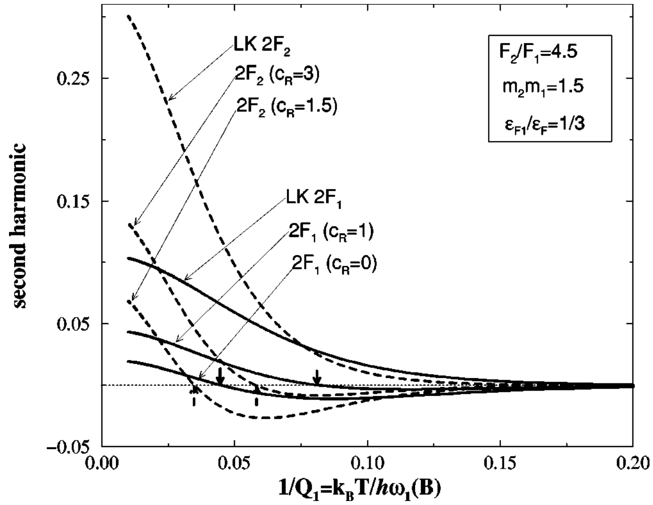

FIG. 6. Second harmonics versus temperature and magnetic field in the two 2D band electron system without and with a reservoir of background states of various strength c_R. The second harmonics of the low fundamental frequency [designated as $h_2^{(F_1)}(Q_1)\rightarrow 2F_1$] are shown by solid lines for $c_R=0$ (without reservoir) and $c_R=1$. Those belonging to the high fundamental frequency [$h_2^{(F_2)}(Q_2)\rightarrow 2F_2$] are shown by dashed lines for reservoir of moderate strength $c_R=1.5$ and $c_R=3$. The standard LK second harmonics ($c_R\rightarrow\infty$) [designated as $(\varepsilon_{F1}/\varepsilon_F)\tilde{m}_2(Q_1)\rightarrow\text{LK}2F_1$ and $\tilde{m}_2(Q_2)\rightarrow\text{LK}2F_2$] are also shown. Note that in certain temperature/magnetic field intervals the second harmonics have opposite signs traversing the zero value. Zeros of the second harmonics appearing in electron systems with and without reservoirs, are shown by arrows.

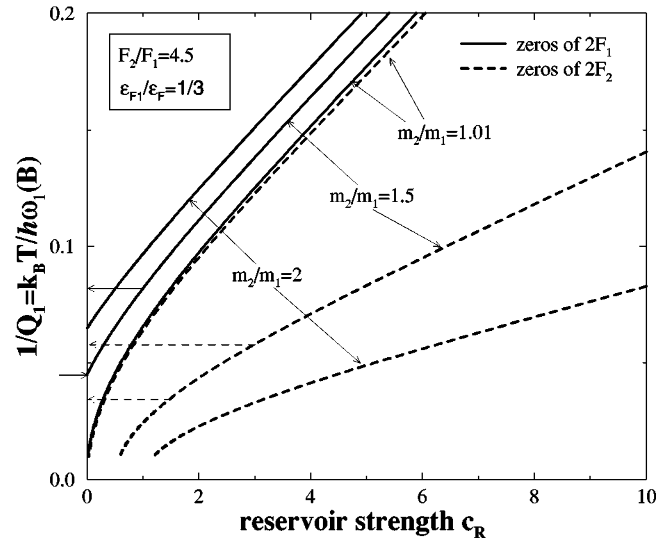

FIG. 7. Temperature and magnetic field of zeros of the second harmonics $2F_1$ and $2F_2$ of the low F_1 and high F_2 fundamental frequencies versus strength of reservoir of background states. Three pairs of sets corresponding to mass ratio $m_2/m_1=1.01,1.5,2$ are presented. The range of temperature and magnetic field corresponds to $Q_1\equiv k_BT/\hbar\omega_1(B)=5-100$. Temperature and magnetic fields, corresponding to zeros of the second harmonics for electron systems with mass ratio $m_2/m_1=1.5$ and reservoir strengths presented in Fig. 6 ($c_R=0,1,1.5,3$), are shown for low fundamental frequency by solid arrows, for high fundamental frequency by dashed arrows (all arrows shown correspond to the arrows in Fig. 6). Note the appearance of second harmonic zeros in the two 2D band system without a reservoir ($c_R=0$).

cur in the electronic 2D system containing a single quantized band and a reservoir of background states in Ref. 15. The second harmonics $2F_1$ and $2F_2$ are shown in Fig. 6.

Note the nonmonotonic behavior of the absolute value of the renormalized second harmonics in comparison to monotonic LK harmonics. We see that at certain temperatures and magnetic fields the second harmonics even traverse the zero value reflecting the symmetric wave form of the corresponding oscillations. Note that the "weight factor" of the first 2D band ($\varepsilon_{F1}/\varepsilon_F=1/3$) relatively diminishes the second harmonics of the low fundamental frequency F_1. Note also that the zeros of the second harmonics are independent of the weight factor [see Eqs. (32), (33)].

It is remarkable that the nonstandard behavior of the second harmonics, nonmonotonic behavior including the appearance of zeros at certain temperatures and magnetic fields is also inherent in multiband electron systems without a reservoir of background states [see the second harmonic of the low fundamental frequency $2F_1(c_R=0)$ in Fig. 6]. This property is analogous to the symmetrization effect that was revealed in an electron system consisting of a single 2D band plus a reservoir [see Ref. 15, where the correlation between the symmetric wave form and the second harmonics zeros has been underlined, see also Ref. 20, where the effect of the symmetrization of magnetic oscillation wave forms due to the background states (represented by the states in 1D band producing open Fermi surface sheet) was first discovered at reservoir strength $c_R=1$ (see also numerical calculation in Ref. 21)]. Some indications on the nonstandard behavior of the second harmonics can be traced in Refs. 6,19, and 9.

The temperatures and magnetic fields where zeros of the second harmonics occur, dependent of the strength of background reservoir states (measured by transfer parameter c_R), are shown in Fig. 7. In contrast to the single band system with a reservoir in multiband systems the zeros of the second harmonics are shifted to higher temperatures for the same strength of reservoir, manifesting the additive interband influence on the effect of symmetrization of the magnetic quantum oscillation wave forms. The same effect of symmetrization occurs in multiband electron systems without a reservoir reflected by the appearance of second (even) harmonics zeros at certain temperatures and magnetic fields (presented in Fig. 7 by crossings of the curves with the ordinate axis $c_R=0$). We see that for the same reservoir strength or in the absence of a reservoir the zeros of the second harmonics corresponding to low and high fundamental frequencies expand from each other with increasing mass ratio m_2/m_1. In pure multiband systems (without reservoir, $c_R=0$) the effect of the symmetrization of wave forms does not occur in all fundamental periods. We see that for two 2D systems without a reservoir at mass ratio $m_2/m_1\gtrsim 1.5$ only the wave forms of oscillations corresponding to low fundamental frequency F_1 are symmetrized. The second harmonic $2F_1$ has zeros, but $2F_2$ does not for mass ratio m_2/m_1

$=1.5,2$ at temperatures and magnetic fields corresponding to $Q_1 \leqslant 100$ [see also the asymmetric sawtooth wave form corresponding to oscillations with high fundamental frequency F_2 in Fig. 2(a) for a system without reservoir $c_R=0$]. Further presentation and discussion of second harmonics properties in multiband electron systems depending on reservoir of background states of various strength c_R can be seen in and after Fig. 9 in the following subsection.

3. Combination harmonics

Now we will write down the expressions for the harmonic amplitudes of combination frequencies:

$$\frac{M_{j_2F_2 \pm j_1F_1}}{M_0} = \frac{(-1)^{j_1+j_2}\pi}{2(1+m_2/m_1+c_R)}\left(\frac{\varepsilon_{F1}}{\varepsilon_F}j_1 \pm \frac{m_2}{m_1}j_2\right) \times \tilde{m}_{j_1}(Q_1)\tilde{m}_{j_2}(Q_2), \quad j_1,j_2=1,2,\ldots, \tag{34}$$

where a plus sign stands for the right-hand-side satellites of the high fundamental frequency $(F_2, j_2=1)$ and its harmonics $(j_2F_2,\ j_2=2,3,\ldots)$ and the minus sign stands for the left-hand-side satellites. It is clear, however, that these expressions are correct for small numbers $j_s=1,2$ for electron systems with weak strength of reservoir $c_R \ll 1$ [see the conditions for the validity of the whole theory of combination frequencies (28)]. The situation improves for electron systems with strong reservoir $(c_R \gg 1)$ but the magnitude of combination harmonics decreases dramatically in this case. The expressions for Fourier harmonics of combination frequencies, Eqs. (34), are coinciding with those written down in the Ref. 22 in the frameworks of the same method that is used in this article, i.e., in the linear approximation on chemical potential oscillations in the expression for oscillating magnetization (22).

The ratio of satellites amplitudes of the high fundamental frequency F_2 and its harmonics disposed on the equal distances from F_2 at the left and the right side [i.e., the $(-)$ and $(+)$ satellites have the same j_1)] is independent of temperature, magnetic field, and the presence of reservoir of background states:

$$\frac{M_{j_2F_2 - j_1F_1}}{M_{j_2F_2 + j_1F_1}} = \frac{j_2(F_2/F_1)-j_1}{j_2(F_2/F_1)+j_1}, \quad j_1,j_2=1,2,\ldots. \tag{35}$$

In the derivation of this expression the relation for parabolic bands were used: $\varepsilon_{F1}/\varepsilon_F=(F_1m_2/F_2m_1)$ [see Eq. (26)]. This expression is independent of the transfer parameter in the limits of the fulfillment of the criterion [Eq. (28)], i.e., in the range where the chemical potential oscillations are small enough. Hence, the above expressions have a limited application constrained by high temperatures, low magnetic fields, and a relatively strong reservoir of background states.

The first satellites of high fundamental frequency F_2 (harmonics of combination frequencies F_2-F_1 and F_2+F_1) for two 2D band systems without a reservoir and with reservoirs with strengths corresponding to $c_R=1$ and $c_R=10$ are presented in Fig. 8. It is seen that the combination harmonics increase with the increase of the chemical potential oscillations, i.e., for weaker reservoirs of background states unable to pin the chemical potential to the Fermi level at all magnetic fields.

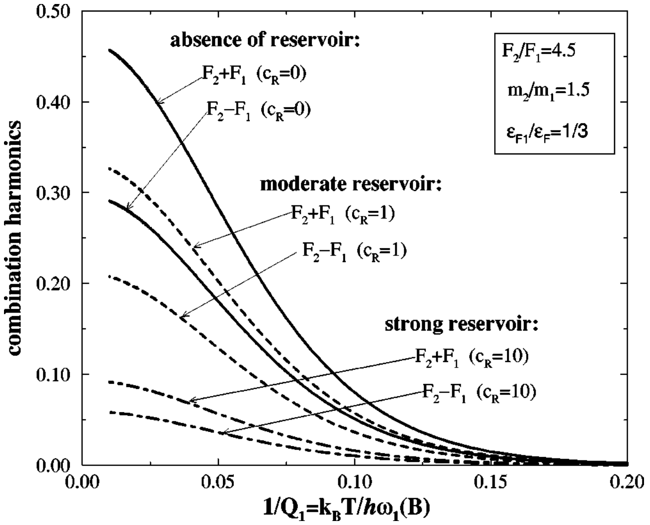

FIG. 8. First satellites of the first harmonic of high fundamental frequency F_2 (harmonics of combination frequencies F_2-F_1 and F_2+F_1) versus temperature/magnetic field for two 2D band electron systems: in the absence of reservoir ($c_R=0$, solid curves) and with a reservoir of moderate ($c_R=1$, dashed curves) and strong ($c_R=10$, dot-dashed curves) strengths. Note that the reservoir suppresses combination harmonics.

The ratio of the first satellites of the high frequency F_2 to the first LK harmonic of the low frequency F_1 in the absence of a reservoir $(c_R=0)$ is

$$\frac{M_{F_2 \pm F_1}/M_0}{(\varepsilon_{F1}/\varepsilon_F)\tilde{m}_1(Q_1)} = \frac{2\pi^2 k_B T m_2(F_1 \pm F_2)}{F_1(m_1+m_2)\hbar\omega_1 \sinh(2\pi^2/Q_2)},$$

which coincides with a similar relation obtained in the framework of the free energy calculation in Ref. 7 (see their Fig. 1).

Finally, we represent in Fig. 9 the comparison of combination and second harmonics for an electron system consisting of two 2D bands with reservoirs of background states of various strengths at a fixed temperature/magnetic field ratio corresponding to $Q_1=20$. We see the monotonic decrease of combination harmonics and a monotonic increase of second harmonics with an increase of the strength of background states. Around $c_R \sim 10$ there is a crossover from dominating combination harmonics to prevailing of second harmonics. The combination harmonics asymptotically disappear while second harmonics approach their corresponding LK values for electron systems with large reservoir strength c_R.

The exact calculations of the Fourier harmonics spectrum for two 2D band systems without a reservoir $(c_R=0)$ presented in Fig. 4(a) and with a reservoir of strength $c_R=1$ in Fig. 4(b) yields that at $Q_1=20$ the second harmonic of the

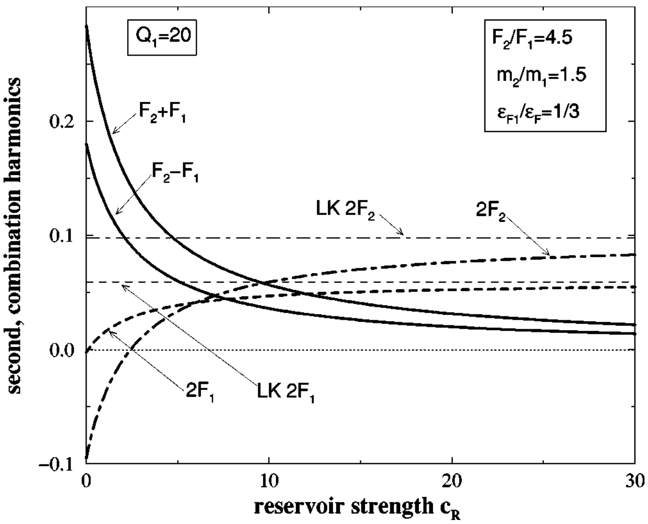

FIG. 9. Second harmonics of low F_1 and high F_2 fundamental frequencies and combination harmonics (first satellites of the first harmonic) of high fundamental frequency F_2 (F_2-F_1 and F_2+F_1) versus reservoir strength c_R at temperatures and magnetic fields corresponding to temperature smoothing parameter $Q_1=\hbar\omega_1(B)/k_BT=20$. The second harmonic of low frequency $2F_1$ and the corresponding second LK harmonic (designated as LK $2F_1$) are shown by dashed lines, those belonging to high frequency ($2F_2$ and LK $2F_2$) by dot-dashed lines. The combination harmonics F_2-F_1 and F_2+F_1 are shown by solid lines. Note the corresponding asymptotic behavior of harmonics at large reservoir strength and crossovers in the region around $c_R\sim 10$.

high fundamental frequency is $|2F_2(c_R=0)|<|2F_2(c_R=1)|$, which contradicts the monotonic behavior of the negative values of this second harmonic $2F_2$ as a function of c_R in the region of small $c_R\leqslant 1$ (see Fig. 9, curve $2F_2$). A similar nonmonotonic behavior at small reservoir strength at ultralow temperatures has been revealed in a model of a single 2D band with reservoir [in Ref. 15, where exact analytical calculations of Fourier harmonics have been performed and demonstrated in Fig. 3, curve 2 (second LA harmonic) in the region $c_R<1$]. Obviously, in calculations of the second harmonic of high fundamental frequency $2F_2$ in the considered model at small $c_R\leqslant 1$ and in a low-temperature–high-magnetic-field region (large Q_1) the restriction by the second order terms on LK harmonics in the expression of $2F_2$ is insufficient [neglection by the higher order terms becomes unjustified: see Eq. (33) and the criterion of its validity, Eq. (28), in the following discussion].

For the second harmonic of the low frequency $2F_1$ the criterion [Eq. (28)] is much easier to fulfill at $c_R\rightarrow 0$ and large Q_1 and, really, the calculations using Eq. (32) and the exact one provide the same results [confer $2F_1$ at $Q_1=20$ for two 2D band system without ($c_R=0$) and with reservoir ($c_R=1$) from Figs. 4(a), 4(b) (exact calculations), Fig. 6 (at $Q_1=20$) and Fig. 9 which are in complete compliance].

IV. CONCLUSION

Usually the Fourier spectrum of magnetoquantum oscillations is analyzed by the Lifshitz-Kosevich formula which rigorously speaking is applicable for independent fundamental frequencies, which is the case where an extremely strong reservoir of background states pins the chemical potential oscillations. Generally, magnetoquantum oscillations due to different parts of the Fermi surface (containing closed and open sheets) are interconnected by oscillations of the chemical potential via exchange of electrons between various orbits in conditions of the thermal equilibrium. Here we have quantitatively investigated the influence of the background states on the wave form and Fourier harmonics of a multiband 2D metal, having a multisheet Fermi surface, at arbitrary temperature and strength of reservoir.

The most striking changes undergo the second harmonics of the fundamental low and high frequencies. First of all, they nonmonotonically depend on either temperature or magnetic field in contrast to the monotonic dependence of standard Lifshitz-Kosevich harmonics. Secondly, depending on the strength of background states they can traverse through zero values, characterizing the most symmetric wave forms of oscillations. In multiband systems zeros of second harmonics occur at higher temperatures due to interband influence, as compared to the single band system with the same reservoir strength. It looks as if the exchange of electrons between 2D bands produce the same symmetrization effect on wave forms of magnetoquantum oscillations as reservoirs in single 2D band systems.[15] At temperatures and magnetic fields where second harmonics zeros occur, the first harmonics and satellites of the high fundamental frequency (harmonics of combination frequencies) dominate the entire Fourier spectrum even at extremely low temperatures where the Lifshitz-Kosevich second harmonics (and higher) should be mostly substantial.

It is remarkable that the effect of symmetrization of oscillation wave forms and the corresponding behavior of second (even) harmonics of the Fourier spectrum is also inherent in multiband electron systems without a reservoir of background states. This effect is due to the interference between different 2D bands via the exchange of electrons in the course of chemical potential oscillations.

Obviously, the developed theory is applicable to 2D multiband electron systems with any number of bands, admitting electron and hole pockets and any kind of reservoir of background magnetically unperturbed states. However, with the increase of the number of bands their total mass factor $\Sigma_s(1/\hbar\omega_s)\sim\Sigma_s m_s$ and transfer parameter c_R will increase, eliminating the chemical potential oscillations [see Eqs. (14), (18)] and the corresponding interconnected effects. The relatively small first satellites of the high frequency (harmonics of the sum and different combination frequencies) observed in USb_2 (Ref. 10) are due to the large mass factor (in the dHvA effect in this compound the deposition from four fundamental frequencies provides $\Sigma_s^4 m_s\approx 16$). The relative magnitudes of the first harmonics of fundamental frequencies depicted in the abovementioned compound is in accordance with our weight factor $\varepsilon_{Fs}/\varepsilon_F$ [note that for parabolic bands $\varepsilon_{Fs}\propto F_s/m_s$, for the expression of magnetization in multiband metals see Eqs. (20), (21].

ACKNOWLEDGMENTS

The discussions with Professor T. Maniv are greatly appreciated. The support of the Center for Absorption in Science, Ministry of Immigrant Absorption, State of Israel (KAMEA Foundation) and the Israel Science Foundation (Israel Academy of Sciences and Humanities) is acknowledged.

---

[1] D. Shoenberg, *Magnetic Oscillations in Metals* (Cambridge University Press, Cambridge, 1984).

[2] J. Wosnitza, *Fermi Surfaces of Low-dimensional Organic Metals and Superconductors* (Springer, Berlin, 1996).

[3] J. Singleton, Rep. Prog. Phys. **63**, 1111 (2000).

[4] A.S. Alexandrov and A.M. Bratkovsky, Phys. Rev. Lett. **76**, 1308 (1996).

[5] A.S. Alexandrov and A.M. Bratkovsky, Phys. Lett. A **234**, 53 (1997).

[6] M. Nakano, J. Phys. Soc. Jpn. **66**, 910 (1997).

[7] A.S. Alexandrov and A.M. Bratkovsky, Phys. Rev. B **63**, 033105 (2001).

[8] A.S. Alexandrov and A.M. Bratkovsky, cond-mat/0207173 (unpublished).

[9] K. Kishigi and Y. Hasegawa, Phys. Rev. B **65**, 205405 (2002).

[10] D. Aoki, P. Wisniewski, K. Miyake, N. Watanabe, Y. Inada, R. Settai, E. Yamamoto, Y. Haga, and Y. Onuki, Philos. Mag. B **80**, 1517 (2000).

[11] E. Ohmichi, Y. Maeno, and T. Yshiguro, J. Phys. Soc. Jpn. **68**, 24 (1999).

[12] Y. Yoshida, A. Mukai, K. Miyake, N. Watanabe, R. Settai, Y. Onuki, T.D. Matsuda, Y. Aoki, H. Sato, Y. Miyamoto, and N. Wada, Physica B **281-282**, 959 (2000).

[13] R.A. Shepherd, M. Elliott, W.G. Herrenden-Harker, M. Zervos, P.R. Morris, M. Beck, and M. Ilegems, Phys. Rev. B **60**, R11 277 (1999).

[14] M.A. Itskovsky, T. Maniv, and I.D. Vagner, Phys. Rev. B **61**, 14 616 (2000).

[15] M.A. Itskovsky and T. Maniv, Phys. Rev. B **64**, 174421 (2001).

[16] M.A. Itskovsky, Eur. Phys. J. B **23**, 283 (2001).

[17] I.M. Lifshitz and A.M. Kosevich, Zh. Éksp. Teor. Fiz. **29**, 730 (1955) [Sov. Phys. JETP **2**, 636 (1956)].

[18] D. Shoenberg, J. Low Temp. Phys. **56**, 417 (1984).

[19] M. Nakano, Phys. Rev. B **62**, 45 (2000).

[20] M.A. Itskovsky, T. Maniv, and I.D. Vagner, Z. Phys. B: Condens. Matter **101**, 13 (1996).

[21] N. Harrison, R. Bogaerts, P.H.P. Reinders, J. Singleton, S.J. Blundell, and F. Herlach, Phys. Rev. B **54**, 9977 (1996).

[22] T. Champel, Phys. Rev. B **65**, 153403 (2002).